

Neutrino oscillation in dark matter with $L_\mu - L_\tau$

Wei Chao,^a Yanyan Hu,^b Siyu Jiang,^a Mingjie Jin,^a

^a*Center for advanced quantum studies, and Department of Physics, Beijing Normal University, Beijing 100875, China*

^b*Key Laboratory of Beam Technology of Ministry of Education, College of Nuclear Science and Technology, Beijing Normal University, Beijing 100875, China*

E-mail: chaowei@bnu.edu.cn, huyy@mail.bnu.edu.cn,
jiangsy@mail.bnu.edu.cn, jinmj@bnu.edu.cn

ABSTRACT: In this paper, we study the phenomenology of a Dirac dark matter in the $L_\mu - L_\tau$ model and investigate the neutrino oscillation behavior in the dark halo. Since dark matter couples to muon neutrino and tau neutrino with opposite sign couplings, it contributes effective potentials, $\pm A_\chi$, to the evolution equation of the neutrino flavor transition amplitude, which can be significant for high energy neutrino oscillations in a dense dark matter environment. We discuss neutrino masses, lepton mixing angles, Dirac CP phase, and neutrino oscillation probabilities in the dark halo using full numerical calculations. Results show that neutrinos can endure very different matter effects. When the potential A_χ becomes ultra-large, three neutrino flavors decouple from each other.

Contents

1	Introduction	1
2	The $U(1)_{L_\mu-L_\tau}$ model	2
2.1	neutrino masses	3
2.2	muon g-2	3
2.3	stability of the Z' , ϕ and χ	4
3	dark matter phenomenology	5
3.1	The relic density	5
3.2	The dark matter scattering off electron	6
4	neutrino oscillations	7
5	Discussions	12

1 Introduction

Robust evidences from astrophysical observations point to the existence of cold dark matter (DM), which can not be addressed by the minimal Standard Model (SM) of particle physics. For a DM mass above 1 keV, it behaves as a cold DM [1]. It is well-known that cold DM needs to interact with the SM particles in addition to the gravitational interaction so as to explain the observed relic abundance, but how it couples to the SM is still unknown. There are various DM candidates with mass ranging from 10^{-22} eV to 10^{55} GeV. Due to the progress of direct and indirect DM detection technology, many DM models have already been excluded, however the neutrino portal [2–12] is relatively safe, as neutrinos themselves are also difficult to probe. One of the most famous neutrino portal model is sterile neutrino DM which can be warm or cold DM and whose production mechanism is via neutrino oscillations [2, 3]. There is also famous scotogenic model [13] which include the DM and neutrino masses into one framework by introducing extra Yukawa interactions. A third typical neutrino portal model takes Z' or dark photon as the mediator [14, 15]. New interactions in the neutrino portal may induce irreducible background, named as “neutrino floor” [16–19], in direct detection experiments. They may also generate some exotic signals in various neutrino oscillation experiments. It is of great significance to study these signals because they may be an important indirect evidence for the existence of CDM.

In this paper, we will study possible signal of DM in neutrino oscillations. As we all know, dark matter accounts for 26.8% of the Universe, and the entire Milky Way Galaxy is in a huge dark halo. When neutrinos propagate in the dark halo, the interaction between neutrinos and DM will lead to the matter effect of neutrino oscillations. Note that the

Particles	ℓ_e	ℓ_μ	ℓ_τ	e_R	μ_R	τ_R	$\chi_{L,R}$	Φ
Charges	0	1	-1	0	1	-1	1	1

Table 1: Particles and relevant $U(1)_{L_\mu-L_\tau}$ charges.

density of DM is about 0.4 GeV/cm^3 [20] near the solar system, so the matter effect caused by DM may be too small to be observed in long baseline neutrino oscillation experiments that are located on the Earth. However, in some regions of the Universe, such as the center of the Galactic center or dwarf spheroidal galaxies, the density of DM can be very high. When high-energy neutrinos pass through these regions, strong matter effect can be induced by the DM. In fact, the matter effect induced by DM has drawn the theorists' attention, and some important issues have already been addressed [21–23]. We will discuss the phenomenology of DM and neutrino oscillations within the framework of $U(1)_{L_\mu-L_\tau}$ [24, 25], which is one of the most economical extensions to the SM. It does not require the introduction of additional elementary particles to eliminate various anomalies. Compared with L_e-L_μ [26], $B-L$ [27], and $U(1)_R$ [28], this model is less restricted and can be used to explain exotic phenomena in high-energy physics experiments, such as the universality violation in the decay of B meson [25] and the low-energy recoil signal of XENON1T [29]. We first perform a systematic study on constraints on the model arising from the observed relic abundance of DM, upper limits on the direct detection cross section as well as the anomalous magnetic moment of the muon. Then we discuss impacts of this new neutral current interaction to neutrino oscillations. In the three-flavor neutrino oscillation scheme, we study the (dark) matter effect of neutrino masses, lepton mixing angles, Dirac CP phase, and neutrino oscillation probabilities in the dark halo using full numerical calculations. Our results are applicable to study high energy neutrino oscillations in a dense dark matter environment.

The remaining of the paper is organized as follows: In section II we introduce the model in detail and discuss various constraints. In section III, we study the phenomenology of DM in the $L_\mu-L_\tau$ model. Section IV is devoted to the study of neutrino oscillations in dark halo. The last part is concluding remarks.

2 The $U(1)_{L_\mu-L_\tau}$ model

It is well-known that [24] the differences of lepton numbers can be gauged $U(1)$ symmetries with anomalies automatically cancelled. Such gauge theories, named as $U(1)_{L_\alpha-L_\beta}$ with $\alpha, \beta = e, \mu, \tau$, have been widely studied as potential candidates of new physics beyond the SM. In this paper, we introduce a vector-like fermion χ in the $U(1)_{L_\mu-L_\tau}$ model to address the DM problem, and study neutrino oscillations in the DM halo. The particles and relevant charge assignments are shown in the table. 1. The Lagrangian for new particles can be written as

$$\mathcal{L} \sim \bar{\chi} i \not{D} \chi + (D_\mu \Phi)^\dagger (D^\mu \Phi) - m_\chi \bar{\chi} \chi + \mu^2 \Phi^\dagger \Phi - \lambda (\Phi^\dagger \Phi)^2 \quad (2.1)$$

where $D_\mu = \partial_\mu - i g_X Z'_\mu$ being the covariant derivative with g_X the new gauge coupling and Z' the new gauge boson, $\Phi \equiv (\phi + i\eta)/\sqrt{2}$ being a complex scalar singlet. When Φ develops

a non-zero vacuum expectation value (VEV) v_Φ , the $U(1)_{L_\mu-L_\tau}$ gauge symmetry is broken spontaneously and Z' gets nonzero mass $M_{Z'} = g_X v_\Phi$. The physical scalar singlet is ϕ with the mass squared $M_\phi^2 = 2\lambda v_\Phi^2$. Here we have assumed that the mixing between Φ and the SM Higgs is negligible for simplicity. In the following we will address several constraints that are relevant to this model.

2.1 neutrino masses

The discovery of neutrino oscillations have proved that the SM is incomplete and one needs to explain the origin of tiny but non-zero neutrino masses. A most economic approach towards understanding the origin of neutrino masses is using the dimension-five Weinberg operator [30],

$$\frac{1}{4}\kappa_{fg}\overline{\ell_{Lc}^C}{}^f\varepsilon_{cd}H_d\ell_{Lb}^g\varepsilon_{ba}H_a + \text{h.c.} \quad (2.2)$$

where f and g are flavor indices, a, b, c and d are isospin indices, H is the SM Higgs doublet, ℓ_L is left-handed lepton doublet. This operator comes from integrating out heavy seesaw particles. In the $U(1)_{L_\mu-L_\tau}$ model, ℓ_L^e , ℓ_L^μ and ℓ_L^τ carry different $U(1)_{L_\mu-L_\tau}$ charges. As a result, the active neutrino mass matrix takes the following form

$$M_\nu \sim \begin{pmatrix} \star & 0 & 0 \\ 0 & 0 & \star \\ 0 & \star & 0 \end{pmatrix}, \quad (2.3)$$

which results in $\theta_{12} = \theta_{13} = 0$ and $\theta_{23} = 45^\circ$ with θ_{ij} the mixing angle of the PMNS matrix in the standard parameterization. This scenario has been ruled out by the neutrino oscillation data. One possible way out is including the following dimension-six effective operators

$$\frac{1}{4}\kappa'_{e\mu}\Phi^\dagger\overline{\ell_{Lc}^C}{}^e\varepsilon_{cd}H_d\ell_{Lb}^\mu\varepsilon_{ba}H_a + \frac{1}{4}\kappa'_{e\tau}\Phi^\dagger\overline{\ell_{Lc}^C}{}^e\varepsilon_{cd}H_d\ell_{Lb}^\tau\varepsilon_{ba}H_a + \text{h.c.} \quad (2.4)$$

Then, only the (2, 2) and (3, 3) elements in the neutrino mass matrix are zero. It has been shown in the Ref. [31] that this kind of texture zero only favors the inverted hierarchy scenario. Actually (2, 2) and (3, 3) elements can be nonzero by introducing dimension-seven effective operators. Taking into account these arbitrariness, we will not concentrate on the flavor structure of neutrino mass matrix in the $U(1)_{L_\mu-L_\tau}$ and take the experimental observables as input in the following study. It should be mentioned that these high dimensional operators may come from integrating out heavy right-handed Majorana neutrinos.

2.2 muon g-2

The anomalous magnetic moment of the muon, $(g-2)_\mu$ is one of the most precisely measured quantities in high energy physics. Its experimental value is [32]

$$a_\mu^{\text{exp}} = 116592089(63) \times 10^{-11}, \quad (2.5)$$

which deviates from the SM prediction [33, 34] by about 3.7σ . Due to the gauge interaction of muon with Z' , a_μ receives contribution from the Z' mediated loop, which can be expressed as

$$\Delta a_\mu = \frac{g_X^2}{4\pi^2} \int_0^1 dt \frac{t^2(1-t)}{t^2 + (1-t)M_{Z'}^2/m_\mu^2} \quad (2.6)$$

As can be seen, both g_X and $M_{Z'}$ are relevant to the Δa_μ , which is always positive in this model. We show in the Fig. 1 contours of Δa_μ in the $M_{Z'} - g_X$ plane. The magenta band is favored by the current data. For more discussions about the $(g-2)_\mu$ in $U(1)_{L_\mu-L_\tau}$, we refer the reader to Refs [35–37] and references cited therein.

2.3 stability of the Z' , ϕ and χ

There are three new particles in the $L_\mu - L_\tau$ model: Z' , ϕ and χ . We will discuss their stabilities one by one. Z' couples to χ , left-handed active neutrinos and charged leptons μ, τ . The total decay rate of Z' to leptons can be written as

$$\Gamma_{Z' \rightarrow \bar{f}f} = \sum_{\alpha=\mu,\tau,\chi} \Theta(M_{Z'} - 2m_\alpha) \frac{\alpha_X M_{Z'}}{3} \sqrt{1 - 4\beta_\alpha} (1 + 2\beta_\alpha) + \frac{M_{Z'} \alpha_X}{3} \quad (2.7)$$

where $\alpha_X = g_X^2/4\pi$ and $\beta_\alpha = m_\alpha^2/M_{Z'}^2$, $\Theta(x)$ is the step function. The second term on the right-handed side of the Eq. (2.7) is the total decay rate to neutrinos in which we have neglected the tiny neutrino masses. For Z' mass smaller than $2m_\nu$ where m_ν is the neutrino mass, the dominate decay channel is to three photons through the muon loop, and the decay rate is calculated as [38]

$$\Gamma_{Z' \rightarrow 3\gamma} \approx \frac{17\alpha^3 \alpha_X}{11664000\pi^3} \frac{M_{Z'}^9}{m_\mu^8} \quad (2.8)$$

where α is the fine-structure constant. In this paper, we assume that $M_{Z'}$ is sizable and thus Z' cannot be a DM candidate.

The physical scalar ϕ arises from the spontaneous breaking of the $U(1)_{L_\mu-L_\tau}$. It only couples to Z' in the toy model. For $M_\phi > M_{Z'}$, ϕ can decay into Z' pair, with the decay rate

$$\Gamma_{\phi \rightarrow Z'Z'} = \alpha_X \frac{M_{Z'}^2}{M_\phi} \sqrt{1 - 4\frac{M_{Z'}^2}{M_\phi^2}} \left(\frac{M_\phi^4}{4M_{Z'}^4} - \frac{M_\phi^2}{M_{Z'}^2} + 3 \right) \quad (2.9)$$

For $M_{Z'} < M_\phi < 2M_{Z'}$, the decay channel turns to be $\phi \rightarrow Z'Z'^* \rightarrow Z'\bar{f}f$. With neutrino pairs in the final state, the decay rate can be written as

$$\Gamma(\phi \rightarrow Z'\bar{\nu}\nu) = \frac{\alpha^2 M_\phi}{24\pi} F(x) \quad (2.10)$$

where $x = M_{Z'}/M_\phi$ and [39]

$$F(x) = \frac{3(1 - 8x^2 + 20x^4)}{(4x^2 - 1)^{1/2}} \arccos\left(\frac{2x^2 - 1}{2x^3}\right) - (1 - x^2) \left(\frac{47}{2}x^2 - \frac{13}{2} + \frac{1}{x^2}\right) - 3(1 - 6x^2 + 4x^4) \ln(x). \quad (2.11)$$

For $M_\phi < M_{Z'}$, the possible decay channels of ϕ are to four leptons or six photons mediated by virtual Z' . In this case, the decay rate can only be calculated numerically. In short, ϕ cannot be stable unless it is ultra-light.

As can be seen in Eq.(1), χ is vector-like fermion with respect to the $U(1)_{L_\mu-L_\tau}$, so there is no interaction between χ and Φ . However there can be a Yukawa interaction $Y_\chi \bar{\ell}_L^{\mu} \tilde{H} \chi_R$, which may lead to an unstable χ . We need to introduce a Z_2 symmetry, under which only χ is odd and all other particles are even, to forbid this Yukawa interaction. As a result, χ is a stable DM candidate and only couples to the lepton sector via the gauge portal.

3 dark matter phenomenology

3.1 The relic density

The DM χ can be thermalized with the thermal bath via the gauge interaction in the early Universe and its evolution is described by the Boltzmann equation,

$$\frac{dn_\chi}{dt} + 3Hn_\chi = -\langle\sigma v\rangle((n_\chi)^2 - (n_\chi^{\text{eq}})^2), \quad (3.1)$$

where n_χ is the number density of χ , H is the Hubble constant and $\langle\sigma v\rangle$ is the thermal average of the reduced annihilation cross section. The reduced annihilation cross section are

$$\sigma v(\bar{\chi}\chi \rightarrow \bar{\ell}_\alpha \ell_\alpha) = 8\pi\alpha_X^2 \sqrt{1 - \frac{m_\alpha^2}{m_\chi^2}} \frac{2m_\chi^2 + m_\alpha^2}{(4m_\chi^2 - M_{Z'}^2)^2 + M_{Z'}^2 \Gamma_{Z'}^2}, \quad (3.2)$$

$$\sigma v(\bar{\chi}\chi \rightarrow Z'Z') = \frac{4\pi\alpha_X^2(1 - M_{Z'}^2/m_\chi^2)^{3/2}}{m_\chi^2(2 - M_{Z'}^2/m_\chi^2)^2}, \quad (3.3)$$

where m_α denotes lepton mass. For the annihilation into neutrinos, one needs to include an extra factor of 1/2 in the cross section. Note that for $M_\phi + M_{Z'} < 2m_\chi$, an extra channel $\bar{\chi}\chi \rightarrow \phi Z'$ opens up and it complicates our physics picture, so we take the singlet scalar mass to be larger than $2m_\chi$ threshold for the simplicity. The thermal average of the reduced annihilation cross section can be written as $\langle\sigma v\rangle = a + b\langle v^2\rangle + \mathcal{O}(v^4)$, where a and b are the s-wave and p-wave terms, respectively.

By solving the Eq. (3.1), the DM relic density is [40, 41],

$$\Omega_{\text{DM}} h^2 = \frac{2.08 \times 10^9 \text{ GeV}^{-1} x_f}{M_{\text{pl}} \sqrt{g_*(T_f)} (a + 3b/x_f)}, \quad (3.4)$$

where $\langle\sigma_{\text{ann}} v\rangle = a + b/x_f$ and $x_f \equiv m_\chi/T_f$ with T_f being the freeze-out temperature, $g_*(T_f)$ is the total number of effective relativistic degrees of freedom when the DM freezes out, M_{pl} is the Planck mass. The parameter x_f is given by,

$$x_f = \ln \left[c(c+2) \sqrt{\frac{45}{8}} \frac{g M_\chi M_{\text{pl}} (a + 6b/x_f)}{2\pi^3 \sqrt{g_*(x_f)} x_f^{1/2}} \right], \quad (3.5)$$

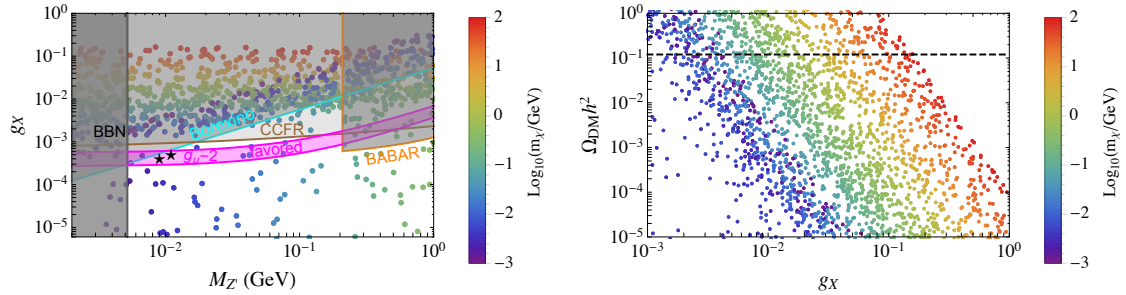


Figure 1: The left panel shows the allowed points in $g_X - M_{Z'}$ plane that may give rise to the observed relic density $\Omega_{\text{DM}}h^2 = 0.12$. The right panel illustrates the correlation between g_X and $\Omega_{\text{DM}}h^2$ as a function of m_χ for $M_{Z'} = 10^{-2}$ GeV.

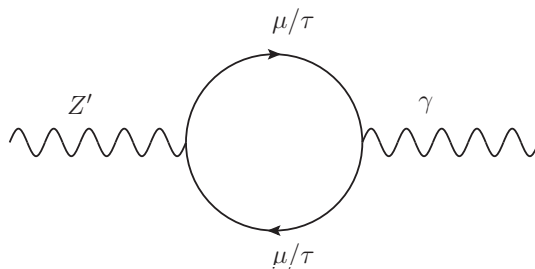


Figure 2: The kinetic mixing between Z' and photon at the one loop with virtual μ and τ leptons [36].

where c is a constant of order one.

In this work, we use **Feynrules** [42] to obtain the model files for the **CalcHeP** [43] and also use the **MicrOMEGAs** [44] to calculate the DM relic density as well as the reduced annihilation cross section. In Fig. 1, we show constraints on the parameter spaces of the model by several physical observables. The plot on the left panel shows the allowed parameter space in the $(M_{Z'}, g_X)$ plane that may give rise to a correct relic density $\Omega_{\text{DM}}h^2 = 0.12$ (scattering points). The gray shadowed regions are already excluded. Among these regions, the black, cyan, brown and orange lines denote constraints from BBN [45, 46], Borexino [45], CCFR [47] and BABAR [48], respectively. The magenta band is the favored region of the muon $g - 2$ [32]. The two black stars denote the reference points to explain IceCube results [45]. For points in the allowed parameter space, we have $m_{Z'} \sim 2m_\chi$, which results in a relatively small g_X as the annihilation cross section is resonantly enhanced. On the right-panel of the Fig. 1 we show the scattering plot of Ωh^2 as the function of the coupling g_X by setting $m_{Z'} = 10^{-2}$ GeV. The black dashed line denotes the observed dark matter relic density. It shows the relic density is inversely proportional to g_X^4 and increases as the increase of m_χ .

3.2 The dark matter scattering off electron

Although the kinetic mixing between Z' and photon is absent at the tree level, the mixing can be generated at the one-loop level by virtual μ and τ leptons [36], as illustrated in the

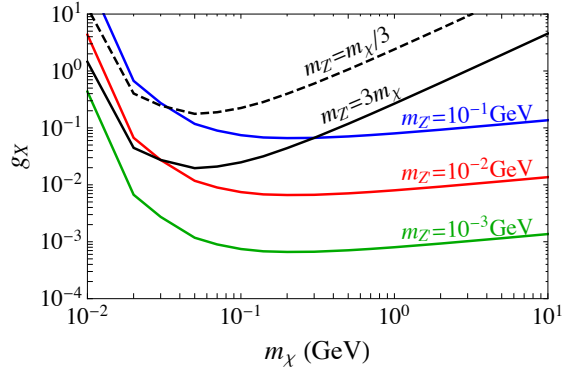


Figure 3: The XENON1T [49] constraints for DM-electron scattering cross section with fixed values of $M_{Z'} = 10^{-1}$ GeV (blue), 10^{-2} GeV (red), 10^{-3} GeV (green) or with $M_{Z'} = m_\chi/3$ (black solid line), $3m_\chi$ (black dashed lines).

Fig. 2,

$$\epsilon = \frac{eg_X}{6\pi^2} \ln\left(\frac{m_\mu}{m_\tau}\right). \quad (3.6)$$

The cross section for the DM scattering off the electron when the momentum transfer is much smaller than the mediator mass $M_{Z'}$ can be written as,

$$\sigma_{\chi e} = \frac{16\pi\epsilon^2\alpha\alpha_X\mu_{\chi e}^2}{M_{Z'}^4}, \quad (3.7)$$

where $\mu_{\chi e}$ is the reduced mass of dark matter and electron.

In Fig. 3, we show in the $m_\chi - g_X$ plane the exclusion limits given by the XENON1T [49] for DM-electron scattering cross section, where the blue, red and green solid lines as well as black solid and dashed lines correspond to $M_{Z'} = 10^{-1}$ GeV, 10^{-2} GeV, 10^{-3} GeV and $M_{Z'} = m_\chi/3$, $3m_\chi$, respectively. This constraint, together with these from low energy precision measurements, puts upper bounds on the new gauge coupling.

4 neutrino oscillations

Neutrino oscillation opens an important window for probing new physics beyond the SM. The neutrino-medium interaction can significantly change the behavior of neutrino oscillations [50, 51]. In addition to the SM charged current and neutral current interactions, there can be other non-standard neutrino interactions which can modify the propagation of neutrinos and thus alter the neutrino oscillation probabilities. For useful reviews see e.g. Refs.[52–54] and references cited therein. In the $L_\mu - L_\tau$ model, the DM-neutrino interaction may induce extra matter effect in neutrino oscillations. We focus on the asymptotic behavior of neutrinos when DM density is large and the ordinary matter effect (i.e., electrons, protons and neutrons) can be ignored, which is similar to the case of dense matter effect [55–57].

When neutrinos propagate in the DM, their evolution equation is modified by the effective potential due to the interactions with the DM through coherent forward elastic

scatterings. The effective potential for muon and tau neutrinos are

$$V_\chi = \pm \frac{g_\chi^2}{m_{Z'}^2} n_\chi, \quad (4.1)$$

with the positive (negative) sign for muon (tau) neutrino, where n_χ is the DM density. The evolution equation of the flavor transition amplitude is

$$i \frac{d}{dx} \Psi_\alpha = \tilde{\mathcal{H}} \Psi_\alpha, \quad (4.2)$$

where $\tilde{\mathcal{H}}$ is the effective Hamiltonian in DM. Given the effective potential in Eq. (4.1), we can write down the effective Hamiltonian $\tilde{\mathcal{H}}$, which differs from the Hamiltonian in vacuum \mathcal{H} , in the flavor basis

$$\tilde{\mathcal{H}} = \mathcal{H} + \mathcal{H}' = \frac{1}{2E} \left[V \begin{pmatrix} m_1^2 & & \\ & m_2^2 & \\ & & m_3^2 \end{pmatrix} V^\dagger + \begin{pmatrix} A_{CC} & & \\ & A_\chi & \\ & & -A_\chi \end{pmatrix} \right], \quad (4.3)$$

where $A_\chi = 2EV_\chi$, $A_{CC} = 2EV_{CC}$ with V_{CC} the effective potential coming from the SM charge current interaction. For neutrinos $A_\chi > 0$ and for anti-neutrinos $A_\chi < 0$. V is the 3×3 unitary Pontecorvo-Maki-Nakagawa-Sakata (PMNS) lepton mixing matrix [58, 59], in which $\theta_{12}, \theta_{13}, \theta_{23}$ are three mixing angles and δ is the Dirac CP phase [60],

$$V = \begin{pmatrix} c_{12}c_{13} & s_{12}c_{13} & s_{13}e^{-i\delta} \\ -s_{12}c_{23} - c_{12}s_{23}s_{13}e^{i\delta} & c_{12}c_{23} - s_{12}s_{23}s_{13}e^{i\delta} & s_{23}c_{13} \\ s_{12}s_{23} - c_{12}c_{23}s_{13}e^{i\delta} & -c_{12}s_{23} - s_{12}c_{23}s_{13}e^{i\delta} & c_{23}c_{13} \end{pmatrix}, \quad (4.4)$$

with $c_{ij} \equiv \cos \theta_{ij}$ and $s_{ij} \equiv \sin \theta_{ij}$ (for $ij = 12, 13, 23$). In our case, the effect of the charged current interaction is ignored ($A_{CC} = 0$) for simplicity. Note that the term proportional to the identity matrix does not affect the neutrino oscillation behaviors, so we can ignore the m_1^2 term, the Hamiltonian $\tilde{\mathcal{H}}$ can be rewritten as,

$$\tilde{\mathcal{H}} = \frac{1}{2E} \left[V \begin{pmatrix} 0 & & \\ & \Delta m_{21}^2 & \\ & & \Delta m_{31}^2 \end{pmatrix} V^\dagger + \begin{pmatrix} 0 & & \\ & A_\chi & \\ & & -A_\chi \end{pmatrix} \right] = \frac{1}{2E} \tilde{V} \begin{pmatrix} \tilde{m}_1^2 & & \\ & \tilde{m}_2^2 & \\ & & \tilde{m}_3^2 \end{pmatrix} \tilde{V}^\dagger, \quad (4.5)$$

where the \tilde{V} is the mixing matrix in DM and the $\tilde{m}_i^2 (i = 1, 2, 3)$ are the eigenvalues. One can obtain $\Delta \tilde{m}_{ji}^2 = \tilde{m}_j^2 - \tilde{m}_i^2$ by solving Eq. (4.5) numerically. The best-fit values of the neutrino oscillation parameters in vacuum are summarized in the Table 2, which are adopted as inputs in following numerical calculations.

We show the modulus of the mass-squared differences $|\Delta \tilde{m}_{21}^2|$ and $|\Delta \tilde{m}_{31}^2|$ as the function of $A_\chi/|\Delta m_{31}^2|$ in the Fig. 4, where plots in the left-panel and right-panel correspond to the normal and inverted mass hierarchies, respectively. It is helpful to discuss the asymptotic behavior of them. When $|A_\chi| \rightarrow 0$, neutrinos are propagating in the "vacuum-dominated" region, and there is almost no DM effect in neutrino oscillations. The DM effect becomes significant for $|A_\chi| \sim |\Delta m_{31}^2|$. While $|A_\chi| \rightarrow \infty$, in other words, $|A_\chi| \gg |\Delta m_{31}^2|$,

	Normal Mass Ordering	Inverted Mass Ordering
θ_{12}	33.82°	33.82°
θ_{13}	8.61°	8.65°
θ_{23}	49.7°	49.7°
δ	217°	280°
$\Delta m_{21}^2 [10^{-5} \text{ eV}^2]$	7.39	7.39
$\Delta m_{31}^2 [10^{-3} \text{ eV}^2]$	2.451	-2.512

Table 2: Three-flavor Oscillation parameters from a global fit data of current experimental data [61]. Note that $\Delta m_{31}^2 < 0$ for (IO).

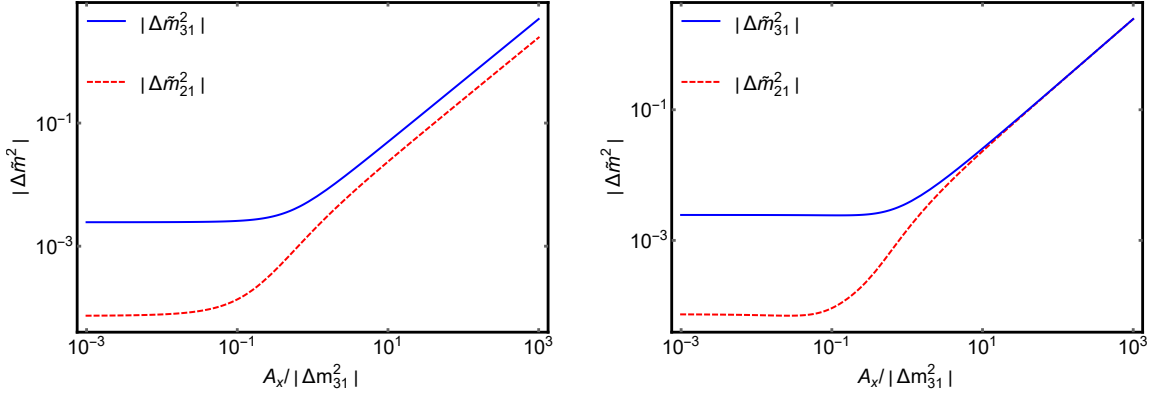


Figure 4: The modulus of the neutrino mass-squared differences in matter $|\Delta\tilde{m}_{21}^2|$ (red and dashed) and $|\Delta\tilde{m}_{31}^2|$ (blue and solid) with respect to $A_\chi/|\Delta m_{31}^2|$ in the normal and inverted mass hierarchies, respectively.

the neutrinos are propagating in the “DM-dominated” region. Three eigenvalues of $\tilde{\mathcal{H}}$ are separated and neutrino oscillation can hardly happen in this region.

In the Fig. 5 and the Fig. 6, we illustrate the evolution behaviors of the matrix elements $|\tilde{V}_{\alpha i}|$, which are derived from the eigenvector-eigenvalue identity [62],

$$|\tilde{V}_{\alpha i}|^2 = \frac{(\lambda_i - \xi_\alpha)(\lambda_i - \zeta_\alpha)}{(\lambda_i - \lambda_j)(\lambda_i - \lambda_k)} = \frac{\lambda_i^2 - \lambda_i(\xi_\alpha + \zeta_\alpha) + \xi_\alpha\zeta_\alpha}{(\lambda_i - \lambda_j)(\lambda_i - \lambda_k)}, \quad (4.6)$$

where $\alpha \in \{e, \mu, \tau\}$, $i, j, k \in \{1, 2, 3\}$ and $i \neq j \neq k$. $\lambda_i/2E$ is the eigenvalue of $\tilde{\mathcal{H}}$. $\xi_\alpha/2E$ and $\zeta_\alpha/2E$ are the eigenvalues of the 2×2 submatrix $\tilde{\mathcal{H}}_\alpha$,

$$\tilde{\mathcal{H}}_\alpha \equiv \begin{pmatrix} \tilde{\mathcal{H}}_{\beta\beta} & \tilde{\mathcal{H}}_{\beta\gamma} \\ \tilde{\mathcal{H}}_{\gamma\beta} & \tilde{\mathcal{H}}_{\gamma\gamma} \end{pmatrix}, \quad (4.7)$$

which is the residual matrix of $\tilde{\mathcal{H}}$ after removing the row α and the column α . It is easy to prove that [62],

$$\xi_\alpha + \zeta_\alpha = (2E)(\tilde{\mathcal{H}}_{\beta\beta} + \tilde{\mathcal{H}}_{\gamma\gamma}) \quad (4.8)$$

$$\xi_\alpha\zeta_\alpha = (2E)^2(\tilde{\mathcal{H}}_{\beta\beta}\tilde{\mathcal{H}}_{\gamma\gamma} - \tilde{\mathcal{H}}_{\beta\gamma}\tilde{\mathcal{H}}_{\gamma\beta}). \quad (4.9)$$

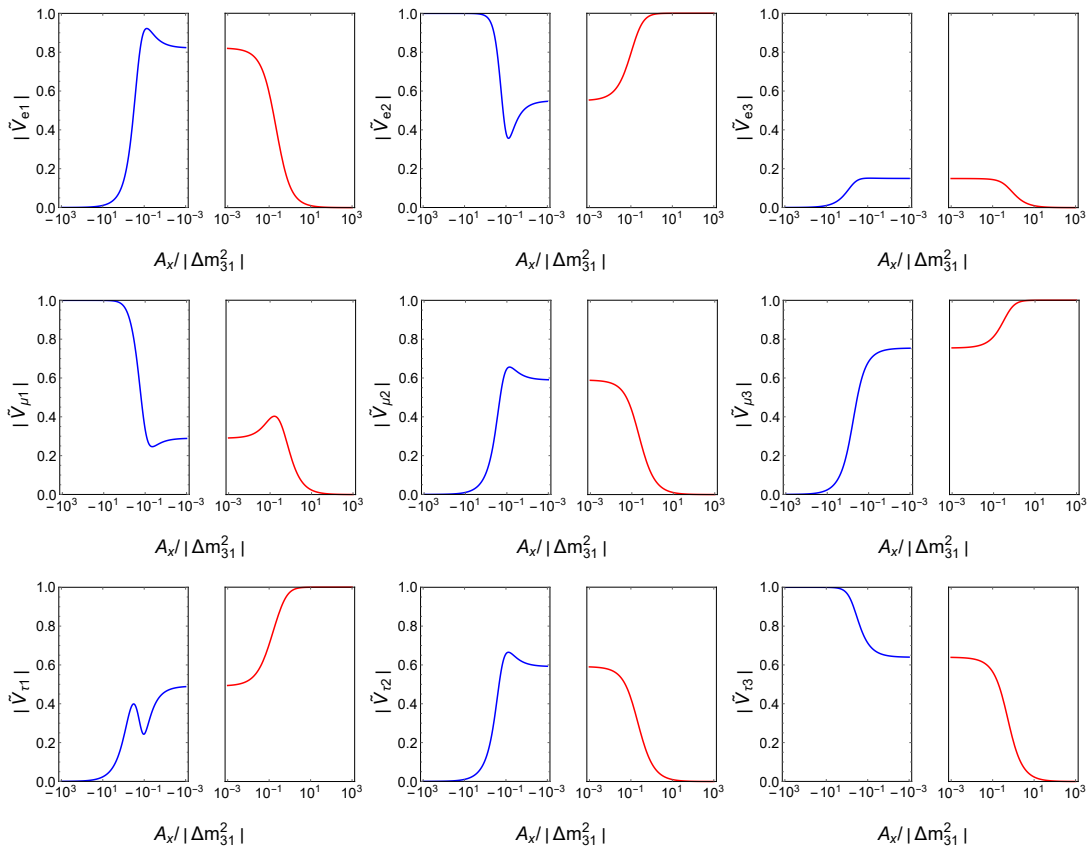


Figure 5: The evolutions of nine effective mixing matrix elements $|\tilde{V}_{\alpha i}|$ (for $\alpha = e, \mu, \tau$, and $i = 1, 2, 3$) with respect to the $A_\chi/|\Delta m_{31}^2|$ in the normal hierarchy for both neutrinos (red, right lines) and anti-neutrinos (blue, left lines).

By substituting Eqs. (4.8) and (4.9) into Eq.(4.6), we can get numerical values of the nine lepton mixing matrix elements in DM. We can conclude from the Fig. 5 and 6 that, corrections to $|\tilde{V}_{\alpha i}|$ are very small for $|A_\chi| \ll |\Delta m_{31}^2|$. $|\tilde{V}_{\alpha i}|$ receive dramatic corrections from the DM when $|A_\chi| \sim |\Delta m_{31}^2|$. For $|A_\chi| \rightarrow \infty$, the neutrino flavors decouple from each other.

Mixing angles in DM can be derived numerically from the PMNS matrix as

$$\tilde{s}_{12} = \frac{|\tilde{V}_{e2}|}{\sqrt{1 - |\tilde{V}_{e3}|^2}}, \quad (4.10)$$

$$\tilde{s}_{13} = |\tilde{V}_{e3}|, \quad (4.11)$$

$$\tilde{s}_{23} = \frac{|\tilde{V}_{\mu 3}|}{\sqrt{1 - |\tilde{V}_{e3}|^2}}, \quad (4.12)$$

where $|\tilde{V}_{\alpha i}|$ are given in the Eq.(4.6).

To get the Jarlskog invariant $\tilde{\mathcal{J}}$ in DM, which is defined as $\mathcal{J} \equiv \text{Im} \left(V_{\alpha i} V_{\beta i}^* V_{\alpha j} V_{\beta j} \right) \times$

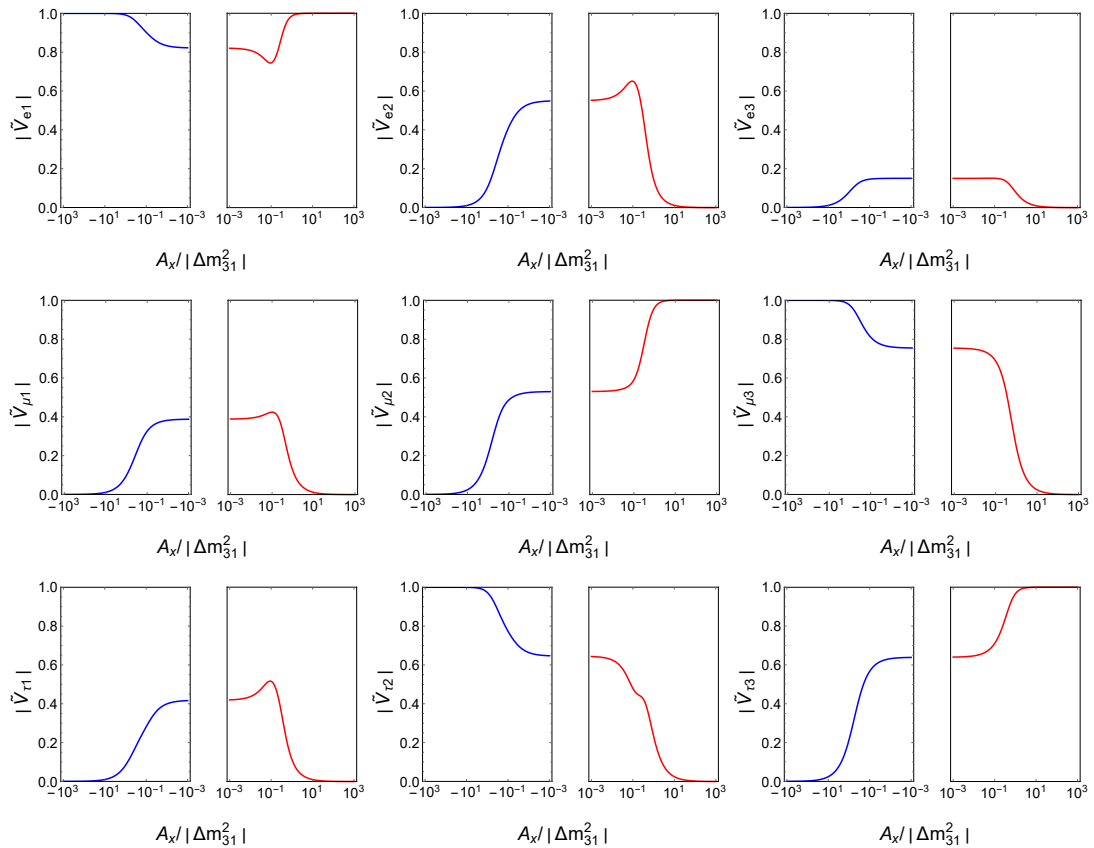


Figure 6: The evolution behaviors of nine effective mixing matrix elements $|\tilde{V}_{\alpha i}|$ (for $\alpha = e, \mu, \tau$, and $i = 1, 2, 3$) with respect to the $A_\chi/|\Delta m_{31}^2|$ in the inverted hierarchy for both neutrinos (red, right lines) and anti-neutrinos (blue, left lines).

$\sum_{\gamma,k} \epsilon_{\alpha\beta\gamma} \epsilon_{ijk}$ (for $\alpha, \beta, \gamma = e, \mu, \tau$ and $i, j, k = 1, 2, 3$) [63, 64], we use the identity in [65],

$$\tilde{\mathcal{J}} \Delta \tilde{m}_{21}^2 \Delta \tilde{m}_{31}^2 \Delta \tilde{m}_{32}^2 = \mathcal{J} \Delta m_{21}^2 \Delta m_{31}^2 \Delta m_{32}^2, \quad (4.13)$$

where $\tilde{\mathcal{J}}$ is the Jarlskog in DM and \mathcal{J} is the Jarlskog in vacuum. The same relationship has been applied to study neutrino oscillations in ordinary matter [66, 67]. The Dirac CP phase δ can be extracted by inserting the explicit expression of Jarlskog,

$$\mathcal{J} = \text{Im}(V_{e1} V_{\mu 1}^* V_{e2}^* V_{\mu 2}) = s_{23} c_{23} s_{13} c_{13}^2 s_{12} c_{12} \sin \delta \quad (4.14)$$

into the Eq. (4.13).

We show the effective Jarlskog invariant in DM $\tilde{\mathcal{J}}$ as the function of $A_\chi/|\Delta m_{31}^2|$ in the Fig.7 for normal hierarchy (left-panel) and inverted hierarchy (right-panel), respectively. We can see that, $\tilde{\mathcal{J}}$ approaches to zero for $|A_\chi| \gg |\Delta m_{31}^2|$, this is because the mixing angle \tilde{s}_{13} tends to zero in this case.

Given all the elements \tilde{s}_{ij} , \tilde{c}_{ij} and the Dirac CP phase $\tilde{\delta}$, we can easily write down the neutrino oscillation probabilities in DM, which is the same as the oscillation probabilities

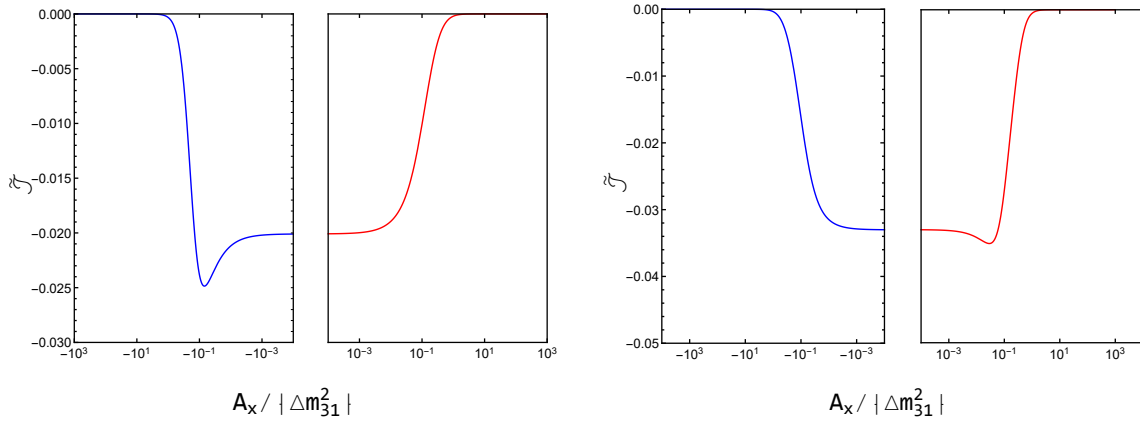


Figure 7: The evolution of the Jarlskog invariant $\tilde{\mathcal{J}}$ in DM with respect to the $A_\chi/|\Delta m_{31}^2|$ in the normal mass ordering and inverted mass ordering for neutrinos (red curves in the right half panel) and anti-neutrinos (blue curves in the left half panel). In the limit $|A_\chi| \rightarrow \infty$, $\tilde{\mathcal{J}}$ approaches to zero.

in vacuum up to replacements $V_{\alpha i} \rightarrow \tilde{V}_{\alpha i}$, $\Delta m_{ji}^2 \rightarrow \Delta \tilde{m}_{ji}^2$ and $\delta \rightarrow \tilde{\delta}$,

$$\begin{aligned} \tilde{P}(\tilde{\nu}_\alpha \rightarrow \tilde{\nu}_\beta) &= \delta_{\alpha\beta} - 4 \sum_{j>i} \text{Re} \left[\tilde{V}_{\alpha i} \tilde{V}_{\beta i}^* \tilde{V}_{\alpha j} \tilde{V}_{\beta j} \right] \sin^2 \tilde{\Delta}_{ji} \\ &\quad \pm 2 \sum_{j>i} \text{Im} \left[\tilde{V}_{\alpha i} \tilde{V}_{\beta i}^* \tilde{V}_{\alpha j} \tilde{V}_{\beta j} \right] \sin 2\tilde{\Delta}_{ji}, \end{aligned} \quad (4.15)$$

where $\tilde{\Delta}_{ji} \equiv \Delta \tilde{m}_{ji}^2 L/4E$ with $\Delta \tilde{m}_{ji}^2 \equiv \tilde{m}_j^2 - \tilde{m}_i^2$ being the effective neutrino mass-squared difference in DM, the Greek letters α, β are the flavor indices run over e, μ, τ , while the Latin letters i, j are the indices of mass eigenstates run over 1, 2, 3. E is the energy of the neutrino/anti-neutrino beam.

As illustrations, we show all nine neutrino oscillation probabilities in DM as the function of $A_\chi/|\Delta m_{31}^2|$ for the normal mass hierarchy in the Fig. 8. We take the parameters listed in the Table. 2 as inputs and set $L/E = 10^4[\text{km}/\text{GeV}]$ when making the plot. We can conclude that the DM effect in neutrino oscillations can be significant for a sizable A_χ , but neutrino oscillation may decouple for an ultra-large A_χ . Note that $n_\chi \sim 0.4 \text{ GeV}/\text{cm}^3$ on the Earth and $\mathcal{O}(g_\chi) \sim 10^{-3}$, it is unlikely to get a large A_χ except for a super high energy neutrino beam. However the DM density can be large in some sub-halo and DM stars can be formed in some asymmetric DM cases, which may result in a large A_χ . Neutrino oscillations in these regions may provide indirect tests to the DM density.

5 Discussions

If dark matter couples to active neutrinos, neutrino properties will be affected by additional matter effects when they are travelling in the DM halo. In this paper, we have introduced an additional neutral current interaction between neutrinos and DM by extending the SM with

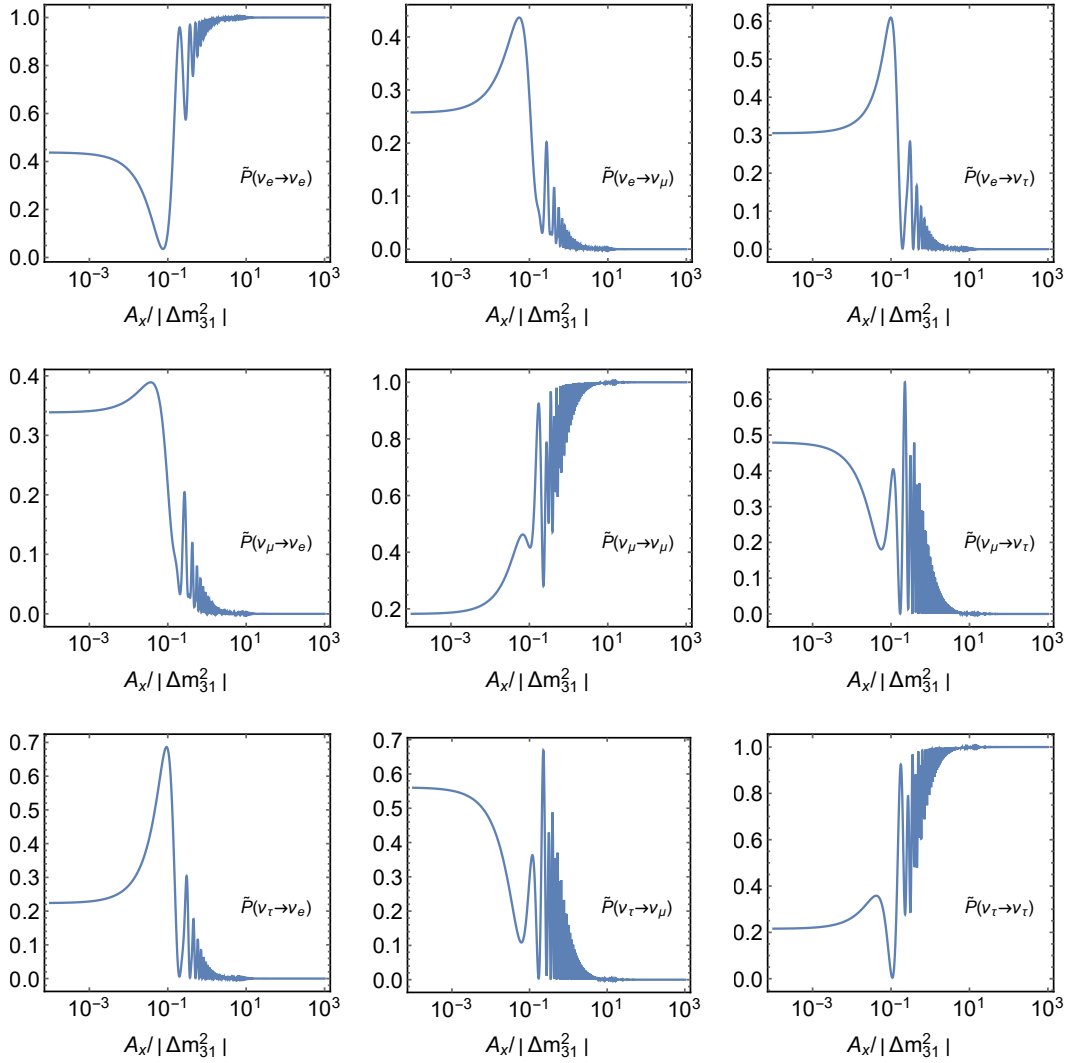


Figure 8: Neutrino oscillation probabilities in DM. In the limit $|A_\chi| \rightarrow \infty$, $\tilde{P}(\nu_e \rightarrow \nu_e)$, $\tilde{P}(\nu_\mu \rightarrow \nu_\mu)$ and $\tilde{P}(\nu_\tau \rightarrow \nu_\tau)$ approach to 1, other channels approach to zero, which means that neutrino is decoherence in this case.

gauged $L_\mu - L_\tau$ symmetry, which introduce an extra effective potential to the evolution equation of the neutrino flavor transition amplitude. We showed that the high energy neutrino oscillations may undergo a matter dominated stage in a dense DM environment, where the neutrino masses, mixing angles as well as neutrino oscillation probabilities are very different compared with oscillation in vacuum. Although it is unable to test the matter effect induced by the DM in long baseline neutrino oscillation experiments as the DM density is too low on the Earth, our results can be applied to evaluate the DM density distribution indirectly by analyzing neutrino oscillation data of known astrophysical sourced neutrino beams.

Acknowledgments

This work was supported by the National Natural Science Foundation of China under grant No. 11775025 and the Fundamental Research Funds for the Central Universities under grant No. 2017NT17.

References

- [1] G. Steigman and M. S. Turner, *Cosmological Constraints on the Properties of Weakly Interacting Massive Particles*, *Nucl. Phys. B* **253** (1985) 375.
- [2] S. Dodelson and L. M. Widrow, *Sterile-neutrinos as dark matter*, *Phys. Rev. Lett.* **72** (1994) 17 [[hep-ph/9303287](#)].
- [3] M. Drewes et al., *A White Paper on keV Sterile Neutrino Dark Matter*, *JCAP* **01** (2017) 025 [[1602.04816](#)].
- [4] W. Chao, *Neutrino Portal via Loops*, [2009.12002](#).
- [5] E. Bertuzzo, S. Jana, P. A. Machado and R. Zukanovich Funchal, *Dark Neutrino Portal to Explain MiniBooNE excess*, *Phys. Rev. Lett.* **121** (2018) 241801 [[1807.09877](#)].
- [6] A. Berlin and N. Blinov, *Thermal neutrino portal to sub-MeV dark matter*, *Phys. Rev. D* **99** (2019) 095030 [[1807.04282](#)].
- [7] M. Becker, *Dark Matter from Freeze-In via the Neutrino Portal*, *Eur. Phys. J. C* **79** (2019) 611 [[1806.08579](#)].
- [8] B. Batell, T. Han, D. McKeen and B. Shams Es Haghi, *Thermal Dark Matter Through the Dirac Neutrino Portal*, *Phys. Rev. D* **97** (2018) 075016 [[1709.07001](#)].
- [9] N. Okada and S. Okada, *Z' -portal right-handed neutrino dark matter in the minimal $U(1)_X$ extended Standard Model*, *Phys. Rev. D* **95** (2017) 035025 [[1611.02672](#)].
- [10] M. Escudero, N. Rius and V. Sanz, *Sterile Neutrino portal to Dark Matter II: Exact Dark symmetry*, *Eur. Phys. J. C* **77** (2017) 397 [[1607.02373](#)].
- [11] M. Escudero, N. Rius and V. Sanz, *Sterile neutrino portal to Dark Matter I: The $U(1)_{B-L}$ case*, *JHEP* **02** (2017) 045 [[1606.01258](#)].
- [12] J. F. Cherry, A. Friedland and I. M. Shoemaker, *Neutrino Portal Dark Matter: From Dwarf Galaxies to IceCube*, [1411.1071](#).
- [13] Y. Farzan and E. Ma, *Dirac neutrino mass generation from dark matter*, *Phys. Rev. D* **86** (2012) 033007 [[1204.4890](#)].
- [14] T. Li and W. Chao, *Neutrino Masses, Dark Matter and B-L Symmetry at the LHC*, *Nucl. Phys. B* **843** (2011) 396 [[1004.0296](#)].
- [15] Y. Cai and W. Chao, *The Higgs Seesaw Induced Neutrino Masses and Dark Matter*, *Phys. Lett. B* **749** (2015) 458 [[1408.6064](#)].
- [16] J. Monroe and P. Fisher, *Neutrino Backgrounds to Dark Matter Searches*, *Phys. Rev. D* **76** (2007) 033007 [[0706.3019](#)].
- [17] L. E. Strigari, *Neutrino Coherent Scattering Rates at Direct Dark Matter Detectors*, *New J. Phys.* **11** (2009) 105011 [[0903.3630](#)].

- [18] J. Billard, L. Strigari and E. Figueroa-Feliciano, *Implication of neutrino backgrounds on the reach of next generation dark matter direct detection experiments*, *Phys. Rev. D* **89** (2014) 023524 [[1307.5458](#)].
- [19] W. Chao, J.-G. Jiang, X. Wang and X.-Y. Zhang, *Direct Detections of Dark Matter in the Presence of Non-standard Neutrino Interactions*, *JCAP* **08** (2019) 010 [[1904.11214](#)].
- [20] J. Read, *The Local Dark Matter Density*, *J. Phys. G* **41** (2014) 063101 [[1404.1938](#)].
- [21] K.-Y. Choi, E. J. Chun and J. Kim, *Neutrino Oscillations in Dark Matter*, *Phys. Dark Univ.* **30** (2020) 100606 [[1909.10478](#)].
- [22] J. Liao, D. Marfatia and K. Whisnant, *Light scalar dark matter at neutrino oscillation experiments*, *JHEP* **04** (2018) 136 [[1803.01773](#)].
- [23] F. Capozzi, I. M. Shoemaker and L. Vecchi, *Neutrino Oscillations in Dark Backgrounds*, *JCAP* **07** (2018) 004 [[1804.05117](#)].
- [24] X.-G. He, G. C. Joshi, H. Lew and R. Volkas, *Simplest Z-prime model*, *Phys. Rev. D* **44** (1991) 2118.
- [25] W. Altmannshofer, S. Gori, M. Pospelov and I. Yavin, *Quark flavor transitions in $L_\mu - L_\tau$ models*, *Phys. Rev. D* **89** (2014) 095033 [[1403.1269](#)].
- [26] G. H. Duan, X.-G. He, L. Wu and J. M. Yang, *Leptophilic dark matter in gauged $U(1)_{L_e - L_\mu}$ model in light of DAMPE cosmic ray $e^+ + e^-$ excess*, *Eur. Phys. J. C* **78** (2018) 323 [[1711.11563](#)].
- [27] P. Langacker, *The Physics of Heavy Z' Gauge Bosons*, *Rev. Mod. Phys.* **81** (2009) 1199 [[0801.1345](#)].
- [28] W. Chao, *Phenomenology of the gauge symmetry for right-handed fermions*, *Eur. Phys. J. C* **78** (2018) 103 [[1707.07858](#)].
- [29] XENON collaboration, E. Aprile et al., *Observation of Excess Electronic Recoil Events in XENON1T*, [2006.09721](#).
- [30] S. Weinberg, *Baryon and Lepton Nonconserving Processes*, *Phys. Rev. Lett.* **43** (1979) 1566.
- [31] D. Meloni, A. Meroni and E. Peinado, *Two-zero Majorana textures in the light of the Planck results*, *Phys. Rev. D* **89** (2014) 053009 [[1401.3207](#)].
- [32] MUON G-2 collaboration, G. Bennett et al., *Final Report of the Muon E821 Anomalous Magnetic Moment Measurement at BNL*, *Phys. Rev. D* **73** (2006) 072003 [[hep-ex/0602035](#)].
- [33] A. Keshavarzi, D. Nomura and T. Teubner, *$g - 2$ of charged leptons, $\alpha(M_Z^2)$, and the hyperfine splitting of muonium*, *Phys. Rev. D* **101** (2020) 014029 [[1911.00367](#)].
- [34] M. Davier, A. Hoecker, B. Malaescu and Z. Zhang, *A new evaluation of the hadronic vacuum polarisation contributions to the muon anomalous magnetic moment and to $\alpha(\mathbf{m}_Z^2)$* , *Eur. Phys. J. C* **80** (2020) 241 [[1908.00921](#)].
- [35] J. Heeck and W. Rodejohann, *Gauged $L_\mu - L_\tau$ Symmetry at the Electroweak Scale*, *Phys. Rev. D* **84** (2011) 075007 [[1107.5238](#)].
- [36] S. Gninenko and N. Krasnikov, *Probing the muon $g - 2$ anomaly, $L_\mu - L_\tau$ gauge boson and Dark Matter in dark photon experiments*, *Phys. Lett. B* **783** (2018) 24 [[1801.10448](#)].

- [37] d. Amaral, Dorian Warren Praia, D. G. Cerdeno, P. Foldenauer and E. Reid, *Solar neutrino probes of the muon anomalous magnetic moment in the gauged $U(1)_{L_\mu-L_\tau}$* , [2006.11225](#).
- [38] J. Redondo and M. Postma, *Massive hidden photons as lukewarm dark matter*, *JCAP* **02** (2009) 005 [[0811.0326](#)].
- [39] W.-Y. Keung and W. J. Marciano, *HIGGS SCALAR DECAYS: $H \rightarrow W^{+-} X$* , *Phys. Rev. D* **30** (1984) 248.
- [40] E. W. Kolb and M. S. Turner, *The Early Universe*, *Front. Phys.* **69** (1990) 1.
- [41] G. Jungman, M. Kamionkowski and K. Griest, *Supersymmetric dark matter*, *Phys. Rept.* **267** (1996) 195 [[hep-ph/9506380](#)].
- [42] A. Alloul, N. D. Christensen, C. Degrande, C. Duhr and B. Fuks, *FeynRules 2.0 - A complete toolbox for tree-level phenomenology*, *Comput. Phys. Commun.* **185** (2014) 2250 [[1310.1921](#)].
- [43] A. Belyaev, N. D. Christensen and A. Pukhov, *CalcHEP 3.4 for collider physics within and beyond the Standard Model*, *Comput. Phys. Commun.* **184** (2013) 1729 [[1207.6082](#)].
- [44] G. Belanger, F. Boudjema, A. Pukhov and A. Semenov, *micrOMEGAs_3: A program for calculating dark matter observables*, *Comput. Phys. Commun.* **185** (2014) 960 [[1305.0237](#)].
- [45] T. Araki, F. Kaneko, T. Ota, J. Sato and T. Shimomura, *MeV scale leptonic force for cosmic neutrino spectrum and muon anomalous magnetic moment*, *Phys. Rev. D* **93** (2016) 013014 [[1508.07471](#)].
- [46] A. Kamada and H.-B. Yu, *Coherent Propagation of PeV Neutrinos and the Dip in the Neutrino Spectrum at IceCube*, *Phys. Rev. D* **92** (2015) 113004 [[1504.00711](#)].
- [47] W. Altmannshofer, S. Gori, M. Pospelov and I. Yavin, *Neutrino Trident Production: A Powerful Probe of New Physics with Neutrino Beams*, *Phys. Rev. Lett.* **113** (2014) 091801 [[1406.2332](#)].
- [48] BABAR collaboration, J. Lees et al., *Search for a muonic dark force at BABAR*, *Phys. Rev. D* **94** (2016) 011102 [[1606.03501](#)].
- [49] XENON collaboration, E. Aprile et al., *Light Dark Matter Search with Ionization Signals in XENON1T*, *Phys. Rev. Lett.* **123** (2019) 251801 [[1907.11485](#)].
- [50] L. Wolfenstein, *Neutrino Oscillations in Matter*, *Phys. Rev. D* **17** (1978) 2369.
- [51] S. Mikheyev and A. Smirnov, *Resonance Amplification of Oscillations in Matter and Spectroscopy of Solar Neutrinos*, *Sov. J. Nucl. Phys.* **42** (1985) 913.
- [52] S. Antusch, J. P. Baumann and E. Fernandez-Martinez, *Non-Standard Neutrino Interactions with Matter from Physics Beyond the Standard Model*, *Nucl. Phys. B* **810** (2009) 369 [[0807.1003](#)].
- [53] T. Ohlsson, *Status of non-standard neutrino interactions*, *Rept. Prog. Phys.* **76** (2013) 044201 [[1209.2710](#)].
- [54] Y. Farzan and M. Tortola, *Neutrino oscillations and Non-Standard Interactions*, *Front. in Phys.* **6** (2018) 10 [[1710.09360](#)].
- [55] Z.-z. Xing, S. Zhou and Y.-L. Zhou, *Renormalization-Group Equations of Neutrino Masses and Flavor Mixing Parameters in Matter*, *JHEP* **05** (2018) 015 [[1802.00990](#)].
- [56] G.-y. Huang, J.-H. Liu and S. Zhou, *Matter effects on the flavor conversions of solar*

- neutrinos and high-energy astrophysical neutrinos*, *Nucl. Phys. B* **931** (2018) 324 [[1803.02037](#)].
- [57] S. Luo, *Neutrino Oscillation in Dense Matter*, *Phys. Rev. D* **101** (2020) 033005 [[1911.06301](#)].
- [58] Z. Maki, M. Nakagawa and S. Sakata, *Remarks on the unified model of elementary particles*, *Prog. Theor. Phys.* **28** (1962) 870.
- [59] B. Pontecorvo, *Neutrino Experiments and the Problem of Conservation of Leptonic Charge*, *Sov. Phys. JETP* **26** (1968) 984.
- [60] PARTICLE DATA GROUP collaboration, M. Tanabashi et al., *Review of Particle Physics*, *Phys. Rev. D* **98** (2018) 030001.
- [61] I. Esteban, M. Gonzalez-Garcia, A. Hernandez-Cabezudo, M. Maltoni and T. Schwetz, *Global analysis of three-flavour neutrino oscillations: synergies and tensions in the determination of θ_{23} , δ_{CP} , and the mass ordering*, *JHEP* **01** (2019) 106 [[1811.05487](#)].
- [62] P. B. Denton, S. J. Parke, T. Tao and X. Zhang, *Eigenvectors from Eigenvalues: a survey of a basic identity in linear algebra*, [1908.03795](#).
- [63] C. Jarlskog, *Commutator of the Quark Mass Matrices in the Standard Electroweak Model and a Measure of Maximal CP Violation*, *Phys. Rev. Lett.* **55** (1985) 1039.
- [64] D.-d. Wu, *The Rephasing Invariants and CP*, *Phys. Rev. D* **33** (1986) 860.
- [65] Z.-z. Xing, *Commutators of lepton mass matrices, CP violation, and matter effects in-medium baseline neutrino experiments*, *Phys. Rev. D* **63** (2001) 073012 [[hep-ph/0009294](#)].
- [66] V. A. Naumov, *Three neutrino oscillations in matter, CP violation and topological phases*, *Int. J. Mod. Phys. D* **1** (1992) 379.
- [67] P. Harrison and W. Scott, *CP and T violation in neutrino oscillations and invariance of Jarlskog's determinant to matter effects*, *Phys. Lett. B* **476** (2000) 349 [[hep-ph/9912435](#)].